JOURNAL OF MATERIALS SCIENCE **36** (2001) 5429–5434

The change of grain boundary internal friction peak during high temperature deformation at different modes

Q. P. KONG*, B. CAI
Institute of Solid State Physics, Chinese Academy of Sciences, 230031 Hefei, People's Republic of China
E-mail: qpkong@mail.issp.ac.cn

G. GOTTSTEIN
Institut für Metallkunde und Metallphysik, RWTH Aachen, 52056 Aachen, Germany

The change of grain boundary internal friction peak during high temperature deformation at different modes (i.e., static tensile creep, cyclic tensile creep, and cyclic reverse torsion) in high purity aluminum was studied in conjunction with microstructure examinations. It was observed that the internal friction peak decreased with increasing plastic strain for all the modes, indicating that grain boundary sliding was degraded by the deformation. Nevertheless, at the same strain the decrement of internal friction was different for different modes, in particular smallest for reverse torsion. The origin of the decrease of internal friction and the difference among different modes is interpreted in the light of microstructure observations.

1. Introduction

The internal friction peak associated with grain boundaries was first observed in Al [1], and later in various metals [2, 3]. The mechanism and the progress of the study of this internal friction peak have been recently reviewed by Kê [4]. It is generally accepted in the literatures that the peak is associated with diffusion controlled anelastic sliding of grain boundaries [1–6].

As a non-destructive tool, the internal friction peak has been used to detect grain boundary segregation and related processes. An investigation of the internal friction in the course of plastic deformation can provide useful information on grain boundary behavior during deformation.

Kong and Dai [7, 8] studied the internal friction peak as a function of creep strain in pure copper at different test conditions, which led to different types of fracture. It was observed that the peak height decreased with increasing strain only slightly (up to 10%) in the course of intergranular fracture, moderately (up to 30%) in the course of mixed fracture, but greatly (up to $\geq$50%) in the course of transgranular fracture. The results indicate that different extent of grain boundary hardening occurs under different types of fracture. A similar effect of creep on the peak was also observed in commercially pure Al (99.6%) [9].

Gottstein and coworkers [10–13] comprehensively studied grain boundary migration and reorientation in Ni and Al during high temperature cyclic deformation. They observed extensive migration and reorientation toward the plane of maximum shear stress. Moreover, grain boundary sliding was evident as revealed by distinct migration steps on the surface during high temperature cyclic tension/compression deformation.

The present paper attempts to use the internal friction as a tool to study the grain boundary behavior during high temperature deformation at different modes in high purity aluminum. It was observed that the internal friction peak decreased with increasing strain for all the modes. Nevertheless, at the same strain the decrement was various for different modes, indicating that the effect of deformation on grain boundary sliding varies with deformation mode. Microstructure examinations were used to elucidate the mechanism of the decrease of internal friction and the different decrement among different modes.

2. Experimental

Internal friction as a function of temperature was measured in air with an automatic inverted torsion pendulum at three frequencies (0.3, 1.0 and 3.1 Hz) in a single cooling process with cooling rate about 4 K/min. The strain amplitude for measuring internal friction was 1×10^{-5}. At first, the internal friction peak was measured prior to deformation, and then after each increment of strain.

The material investigated was Al with 99.999% purity. The specimens were shaped by spark erosion from a cold rolled sheet with thickness of 1.0 mm. The dimensions of the specimens were 55 mm in gauge length and 1.7×1.0 mm^2 in cross section. Before the tests, the specimens were annealed at 450°C for 2 hours. The

*Author to whom all correspondence should be addressed.

average grain size was about 2 mm, i.e., part of the grains had a size larger than the width and thickness of the specimen, and only about 25 grains comprised in the gauge length of a specimen.

The deformation tests were conducted *in situ* at two temperatures and three different modes as follows. (a) The static creep in tension was tested at 450°C, 1.5 MPa; and at 300°C, 4.0 MPa. (b) The cyclic creep in tension was tested at 450°C, 0–1.5 MPa; and at 300°C, 0–4.0 MPa; both with a cyclic period of 30 s, i.e., the stress was periodically changed from zero to the given stress. (c) Cyclic torsion was performed at 450°C and 300°C, both with a cyclic period of 30 s and a reverse torsion angle ±40°, which is equivalent to a minimum shear strain ±0.63% on the surface (see Equation 2 in next section).

After deformation and internal friction measurement at different strains, the specimens were examined by optical metallograph, scanning electron microscopy (SEM), electron backscatter diffraction (EBSD) and transmission electron microscopy (TEM). The SEM and EBSD examinations were carried out in a SEM JSM-6100, and the TEM in a JEM-2000 FXII operating at 200 kV. For post deformation surface observations, part of the specimens were polished and etched before deformation.

3. Results

3.1. Internal friction measurements

At first, the internal friction as a function of temperature was measured before deformation. From the shift of the peak temperature with frequency, the activation energy was measured to be 1.5 eV, which is coincident with that in literature [4].

Fig. 1 shows the internal friction measured at 1.0 Hz after (a) different tensile strains of static creep at 450°C, and (b) different cycles of cyclic reverse torsion at 300°C respectively. Similar results for cyclic creep and cyclic torsion at 450°C, and static creep and cyclic creep at 300°C were also obtained (not shown here).

The internal friction peak was considered to be superimposed by a background Q_b^{-1}, which can be expressed by [2, 14]

$$Q_b^{-1} = A_1 + A_2 \exp(-A_3/kT), \qquad (1)$$

where A_1, A_2 and A_3 are constants.

After subtracting the background according to Equation 1 by using a fitting procedure according to Bevington [15] and Fang [16], the net internal friction peak and the background resolved from the data in Fig 1a and b are plotted in Fig. 2a and b.

Fig. 3a and b show the normalized peak height Q_{md}^{-1}/Q_{mb}^{-1} (i.e., the net peak height after deformation divided by that before deformation) versus the plastic strain ε_p at 450°C and 300°C respectively. The plastic strains for cyclic deformation are defined as follows.

The strain of cyclic creep is the tensile strain at the peak stress before unloading. The strain of cyclic torsion is the cumulative equivalent tensile strain. The equivalent tensile strain per cycle was calculated according to Blum and coworkers [17]:

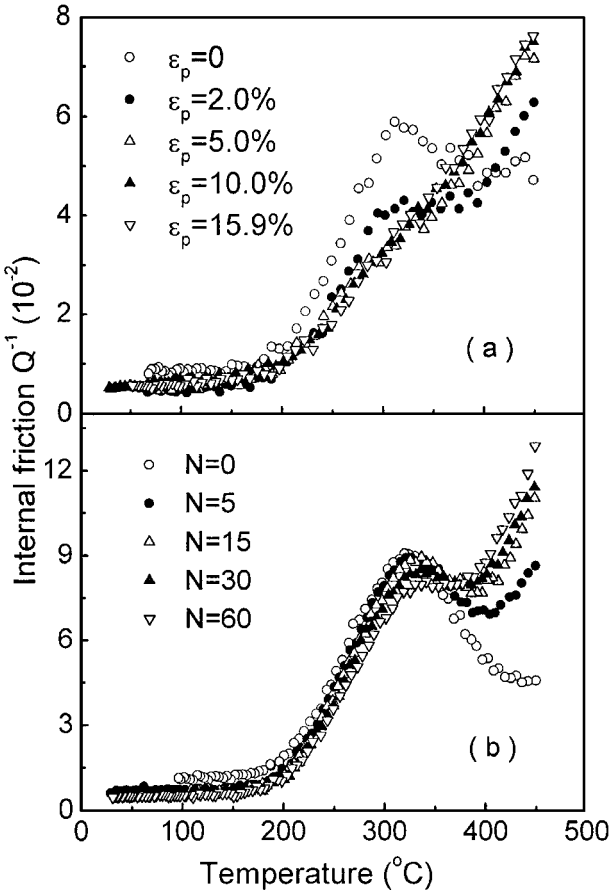

Figure 1 Internal friction of pure Al at 1.0 Hz after: (a) different strains ε_p of static creep at 450°C, 1.5 MPa; (b) different cycles N with torsion angle ±40° at 300°C.

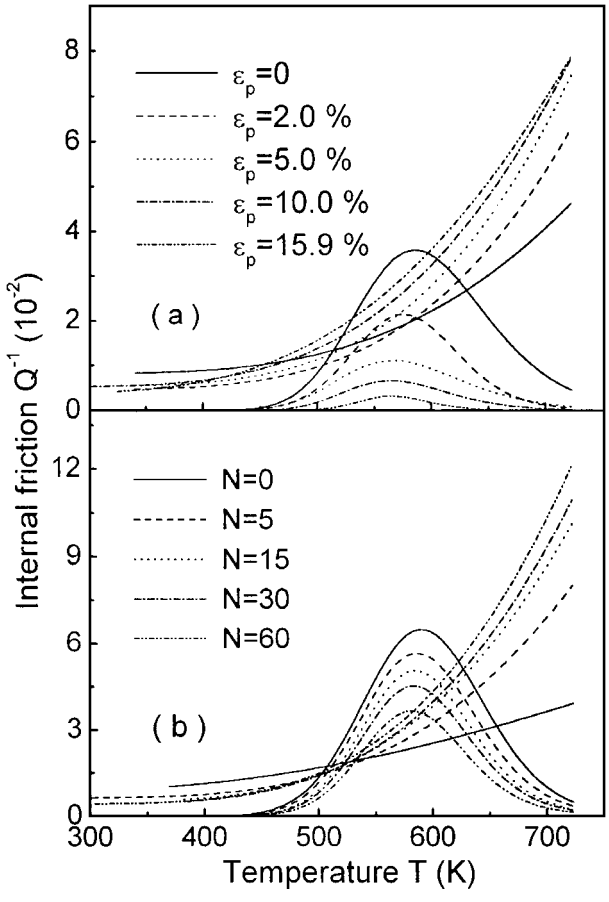

Figure 2 The resolved net peak and background: (a) and (b) correspond to Fig. 1a and b respectively.

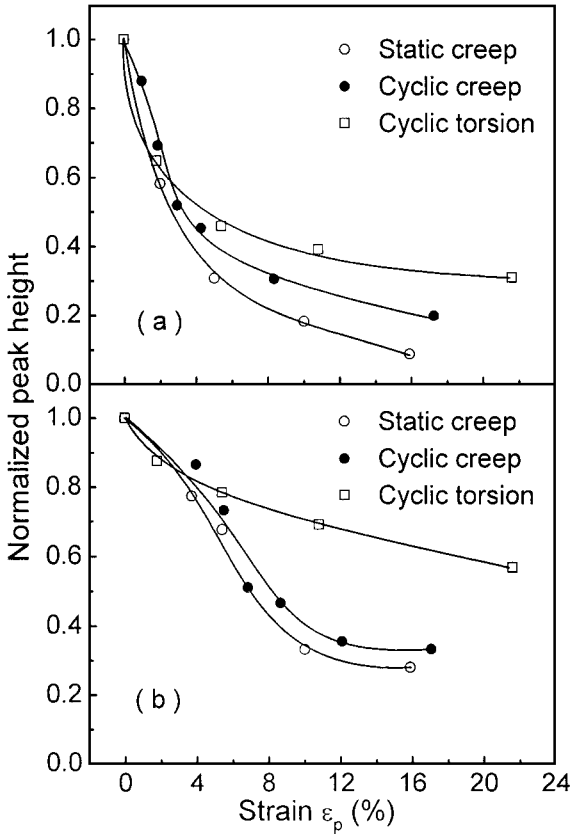

Figure 3 Normalized peak height Q_{md}^{-1}/Q_{mb}^{-1} as a function of plastic strain ε_p for different deformation modes at: (a) 450°C; (b) 300°C.

$$\gamma = w\theta/L, \qquad \varepsilon_p = \gamma/\sqrt{3}, \tag{2}$$

where γ is the shear strain, w is the radial distance from the torsion axis, θ is the torsion angle, L is the gauge length of the specimen, and ε_p is the equivalent tensile strain. The factor $\sqrt{3}$ is the conversion factor from torsion to tension. According to Equation 2, the minimum shear strain at the specimen surface is 0.63%, and the equivalent tensile strain is 0.36% per cycle. The cumulative equivalent tensile strain is 0.36% times the number of torsion cycles N.

It can be seen from Fig. 3 that the internal friction peak decreases with increasing strain at both temperatures, and the decrement at larger strains can exceed 40% for each of the three deformation modes. The decrement is in the range for transgranular or mixed type fracture as indicated in previous papers [7–9]. This phenomenon is in agreement with the observed fracture of high purity Al in this study.

However, there are conspicuous differences among the different deformation modes, as shown in Fig. 3. At the same strain, the decrement of internal friction is largest for static creep, less for cyclic creep, and least for cyclic torsion.

The activation energy and half width of the internal friction peak after different strains were found to be essentially unchanged as compared with those before deformation. Hence the normalized peak height Q_{md}^{-1}/Q_{mb}^{-1} should be equal to ratio of relaxation strengths after and before deformation Δ_d/Δ_b [2–4].

In addition, one can see from Fig. 2a and b that the net internal friction peak not only decreases in height, but also shifts to lower temperature after deformation. The reason will be interpreted together with the decrease of peak height.

It can also be seen from Fig. 2a and b that the high temperature background increases with the increasing strain. It is generally assumed that the background is associated with diffusion controlled relaxation of dislocations [2, 14]. Hence the rise of the background should be associated with an increasing dislocation density and its reconfiguration induced by deformation.

3.2. Microscopic observations

Fig. 4a and b show the surface observations after static creep at 300°C and 450°C respectively. One can see that numerous slip traces intersect the grain boundaries in static creep, and the spacing of slip traces is larger at higher temperature. But the slip traces were less in cyclic creep, and very seldom in cyclic torsion (not shown here).

Fig. 5a and b show the surface observations after cyclic torsion at 300°C and 450°C respectively. In the case of cyclic torsion, distinct migration steps of grain boundaries appear, which is known as a result of combined boundary sliding and migration. The spacing of migration steps is also larger at higher temperature. No

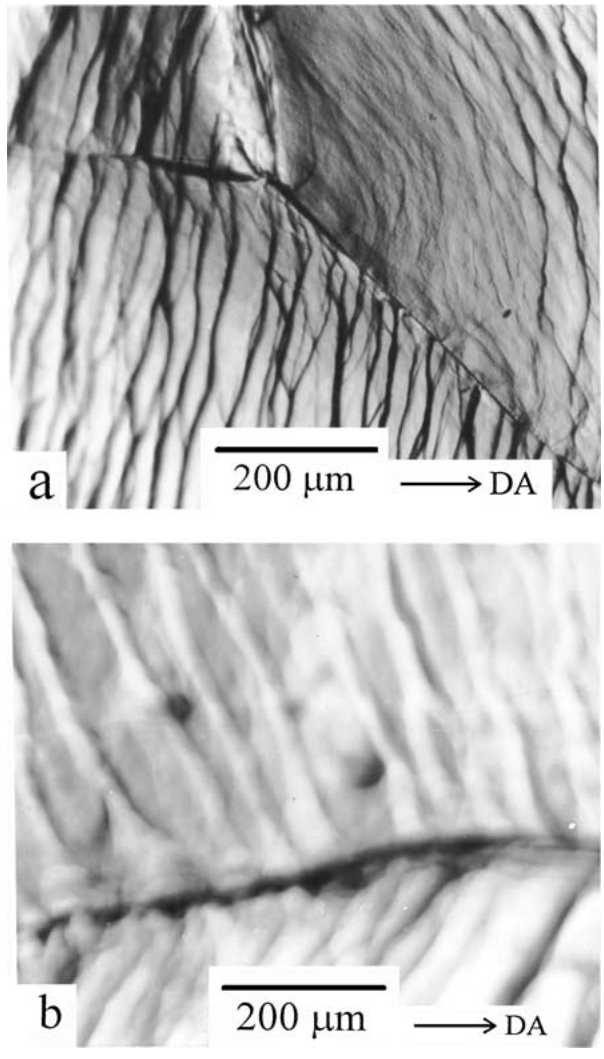

Figure 4 Surface observations of the specimens undergone static creep: (a) at 300°C, $\varepsilon_p = 10\%$; (b) at 450°C, $\varepsilon_p = 10\%$. DA is the deformation axis.

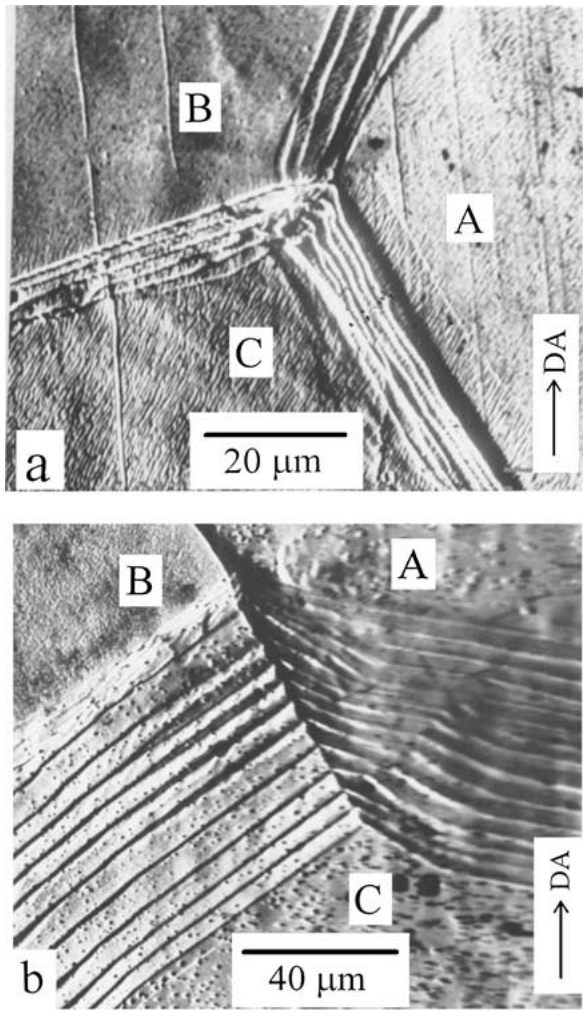

Figure 5 Surface observations of the specimens undergone cyclic torsion: (a) at 300°C, $N = 5$; (b) at 450°C, $N = 15$. DA is the deformation axis.

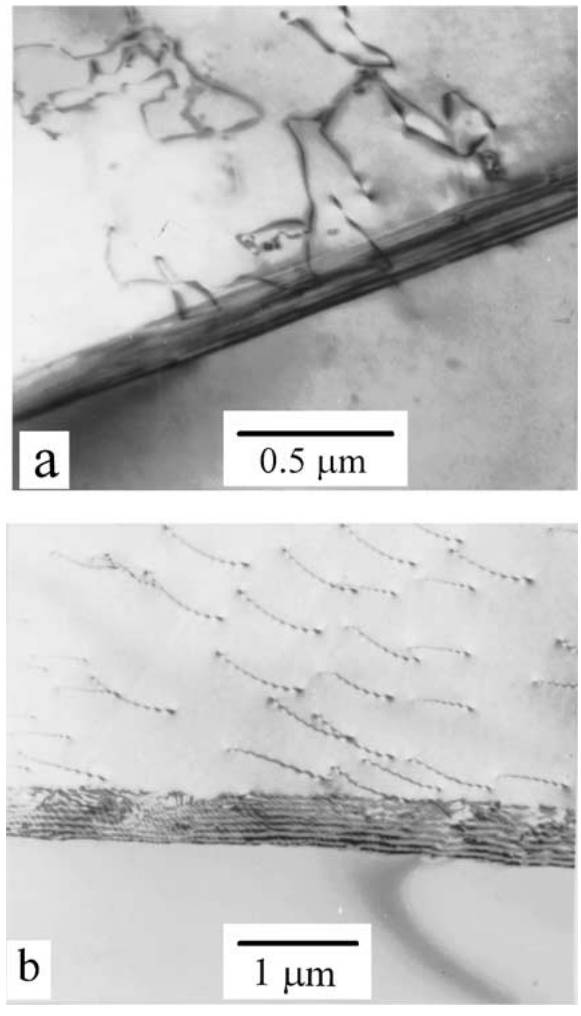

Figure 6 TEM photographs of the specimens undergone: (a) static creep at 450°C, $\varepsilon_p = 5\%$; (b) cyclic torsion at 450°C, $N = 15$.

such migration steps were observed in static creep and cyclic creep, implying a less extent of migration.

It is noted from Fig. 5 that, the number of the migration steps is equal to the number of reverse torsion cycles, which confirms the observations on high purity Al by Yavari and Langdon [18] in reverse bending fatigue, and Weiss and Gottstein [12, 13] in tension/compression fatigue.

The EBSD measurements indicated that in Fig. 5, all the boundaries meeting at the triple junction were original large angle boundaries. In Fig. 5a, the migration directions of boundaries AB, BC and CA were A → B, B → C, and A → C respectively. While in Fig. 5b, the migration directions of boundaries BC and AC were B → C and A → C respectively; no migration step of boundary AB was observed, perhaps owing to its orientation.

Fig. 6 shows two examples of TEM photographs for different deformation modes at the same temperature. It can be seen that many lattice dislocations intersect the grain boundary in static creep (Fig. 6a), but the intersections were less in cyclic torsion and in cyclic torsion. For cyclic torsion (Fig. 6b), individual dislocations are observed to decompose into secondary grain boundary dislocations (SGBDs) in the encountered boundary. The motion of the SGBDs generates a combined sliding/migration displacement of the boundary.

As mentioned above, the different modes of deformation result in characteristic changes of microstructure. The intersections of slip traces and dislocations with grain boundaries are more extensive in static creep, but less in cyclic creep and cyclic torsion. This is not surprising since cyclic creep and cyclic torsion are distinguished from static creep by repeated unloading at elevated temperatures and thus, enhances static and dynamic recovery of its dislocation structure.

In contrast, the migration of grain boundaries occurs most extensively in reverse torsion as obvious from the distinct migration steps. In cyclic torsion, not only unloading but also a reversal of strain is enforced in every cycle, which favors the migration to occur.

Both the intersections of dislocations with boundaries and the migration of boundaries will influence the anelastic sliding of grain boundaries. The intersections of dislocations with grain boundaries cause a perturbation of grain boundary structure, harden the boundaries and hence suppress grain boundary sliding. The migration of grain boundaries facilitates grain boundary sliding by removing the perturbation of grain boundaries.

Correspondingly, monotonic static creep results in the strongest decrement of internal friction, cyclic creep causes less decrement of internal friction, while cyclic torsion keeps up internal friction the most, i.e. the level of internal friction remains high.

4. Discussion

As shown by Kê and other authors, the observed internal friction peak is associated with grain boundaries, since it is absent in single crystals. It is generally accepted that the peak can be attributed to diffusion controlled anelastic sliding of grain boundaries [1–6], although another mechanism has also been suggested [19]. Based on this understanding, the mechanism of the decrease of internal friction with increasing strain as shown in Figs 1–3 will be suggested.

Under the action of an elastic stress τ_a for measuring internal friction, in addition to an instantaneous strain ε_0, an anelastic strain ε_{an} caused by grain boundary sliding occurs. During the sliding, an internal stress is developed by certain constrains (e.g., triple junctions and/or other obstructions) to oppose further sliding until an equilibrium state is reached. The sliding is recoverable. When the applied stress is removed, the boundaries will slide back.

The relaxation strength Δ can be expressed as [2, 7]

$$\Delta = (M_U - M_R)/M_R = (\varepsilon - \varepsilon_0)/\varepsilon_0 = \varepsilon_{an}/\varepsilon_0, \quad (3)$$

where M_U and M_R are unrelaxed and relaxed moduli respectively, ε_{an} is the anelastic strain at its equilibrium, and ε is the summation of ε_0 and ε_{an}.

The relation between equilibrium anelastic strain ε_{an} and average sliding displacement X is [2, 4]

$$\varepsilon_{an} = MX/d, \quad (4)$$

where d is the average grain size, M is an orientation factor, which relates to the spatial distribution of boundary planes with regard to the direction of applied stress for measuring internal friction.

It is obvious from Equations 3 and 4 that the decrease of peak height or relaxation strength means that the average displacement of anelastic sliding along grain boundaries is reduced.

Before deformation, the grain boundaries in an annealed specimen are relatively smooth, so that the anelastic sliding along grain boundaries can take place for a longer distance.

After deformation, a large number of dislocations produced by deformation intersect the grain boundaries. Such intersections will introduce perturbations of grain boundaries to impede the sliding, resulting in a decrease of average displacement of anelastic sliding along grain boundaries.

The average sliding displacement X can be assumed as a function of dislocation density ρ and its configuration

$$X = K/\rho^{1/2}, \quad (5)$$

where $1/\rho^{1/2}$ is the average spacing of dislocations, and K a structural coefficient which depends on dislocation configuration and hence on deformation mode.

The dislocation density ρ increases with progressing plastic deformation ε_p, and this dependency can be expressed by the empirical relation [20]

$$\rho = \rho_0\left(1 + C\varepsilon_p^n\right), \quad (6)$$

where ρ_0 is the dislocation density before deformation, C and n are numerical constants which may be dependent on test condition.

Substituting Equation 5 into Equation 4, we have the equilibrium anelastic strain before deformation

$$\varepsilon_b = \frac{MK}{\rho_0^{1/2}d}. \quad (7)$$

After deformation, the equilibrium anelastic strain becomes

$$\varepsilon_d = \frac{MK'}{\rho^{1/2}d}. \quad (8)$$

Here we assume that the orientation factor M is little changed since the plastic strain in this study is not very large. But the structural coefficient K in Equation 7 is replaced by K' in Equation 8. The ratio of ε_d and ε_b is then

$$\frac{\varepsilon_d}{\varepsilon_b} = \frac{K'}{K}\left(\frac{\rho_0}{\rho}\right)^{1/2}. \quad (9)$$

Substituting Equations 3 and 6 into Equation 9, we have

$$\frac{\Delta_d}{\Delta_b} = \frac{K'}{K\left(1 + C\varepsilon_p^n\right)^{1/2}}. \quad (10)$$

It can be seen from Equation 10 that the relaxation strength or peak height should decrease with the increase of plastic strain ε_p. The different decrement of internal friction at the same strain under different deformation modes can be attributed to the difference in dislocation density (i.e., the constants C and n) and its configuration (i.e., the structural coefficient K'). The mechanism in detail is to be further studied.

Now we turn to the shift of internal friction peak to a lower temperature after deformation, as shown in Fig. 2a and b. Mori and coworkers [6] showed that the decrease of grain boundary sliding displacement should reduce the relaxation strength and the relaxation time by the same factor. Hence τ_d/τ_b should be equal to Δ_d/Δ_b, where τ_d and τ_b are the relaxation times of boundary sliding after and before deformation respectively. It is obvious from Equation 10 that the relaxation time should also decrease with increase of plastic strain. Accordingly the internal friction peak shifts to a lower temperature with increasing strain.

5. Summary and conclusions

The change of grain boundary internal friction peak in the course of high temperature deformation at different modes in high purity Al has been investigated in conjunction with metallography, SEM, EBSD and TEM examinations.

The internal friction peak decreases with increasing plastic strain for all the deformation modes. However, the amount of the decrement of internal friction peak at the same plastic strain is different for different deformation modes. It is the largest in static creep, less in cyclic creep, and least in cyclic torsion.

Microscopic observations reveal that the intersections of slip traces and lattice dislocations with grain boundaries are the most in static creep, but less in cyclic creep and cyclic torsion. The intersections suppress grain boundary sliding, and hence degrade the internal friction. In contrast, the migration of grain boundaries occurs most extensively in cyclic torsion, but less in cyclic creep and static creep. The migration of grain boundaries facilitates grain boundary sliding by removing the perturbation introduced by deformation, and accordingly enhances the internal friction.

The decrease of internal friction caused by deformation is attributed to the decrease of sliding displacement along grain boundaries. The different extent of the decrement of internal friction at the same plastic strain among different deformation modes is possibly associated with the difference in dislocation density and its configuration.

Acknowledgements

This project has been jointly supported by the National Natural Science Foundation of China (Grant 59871049) and the Deutsche Forschungsgemeinschaft. The authors express their gratitude to Ms. D. Mattissen and Dr. W. Hu for the help in microstructure examinations.

References

1. T. S. K Ê, *Phys. Rev.* **71** (1947) 533.
2. A. S. NOWICK and B. S. BERRY, "Anelastic Relaxation in Crystalline Solids" (Academic Press, Inc., New York, 1972).
3. H. GLEITER and B. CHALMERS, "High-Angle Grain Boundaries" (Pergamon Press, Oxford, 1972), ch. 8.
4. T. S. K Ê, *Metall. Mater. Trans. A* **30** (1999) 2267.
5. R. RAJ and M. F. ASHBY, *Metall. Trans.* **2** (1971) 1113.
6. T. MORI, M. KODA, R. MONZEN and T. MURA, *Acta Metall.* **31** (1983) 275.
7. Q. P. KONG and Y. DAI, *Phys. Stat. Sol. A* **118** (1990) 431.
8. Y. DAI, S. M. LIU and Q. P. KONG, *ibid.* **118** (1990) K21.
9. Q. P. KONG and C. C. CHANG, *Acta Physica Sinica* **24** (1975) 168.
10. G. GOTTSTEIN and L. S. SHVINDLERMAN, "Grain Boundary Migration in Metals: Thermodynamics, Kinetics, Applications" (CRC Press, Boca Raton, 1999).
11. D. A. MOLODOV, U. CZUBAYKO, G. GOTTSTEIN and L. S. SHVINDLERMAN, *Acta Mater.* **46** (1998) 553.
12. S. WEISS and G. GOTTSTEIN, *Mater. Sci. Eng., A* **256** (1998) 8.
13. *Idem.*, *Mater. Sci. Tech.* **14** (1998) 1169.
14. J. FRIEDEL, "Dislocations" (Pergamon Press, Oxford, 1964) ch. 11.
15. P. R. BEVINGTON, "Data Reduction and Error Analysis for Physical Sciences" (McGraw-Hill, New York, 1969) p. 235.
16. Q. F. FANG, *Acta Metall. Sinica* **32** (1996) 565.
17. W. BLUM, Q. ZHU, R. MERKEL and H. J. MCQUEEN, *Z. Metallkd.* **8** (1996) 1.
18. P. YAVARI and T. G. LANGDON, *Acta Metall.* **31** (1983) 1595.
19. M. L. NO, C. ESNOUF, J. SAN JUAN and G. FANTOZZI, *ibid.* **36** (1988) 827.
20. C. F. LO, G. J. FENG, W. E. MAYO and S. WEISSMANN, *Mater. Sci. Eng., A* **113** (1989) 219.

Received 29 August 2000
and accepted 8 August 2001